

# Effective Stress Analysis for the Seismic Response of Shallow Foundations on Liquefiable Sand

K.I. Andrianopoulos, G.D. Bouckovalas, D.K. Karamitros & A. G. Papadimitriou

*School of Civil Engineering, Geotechnical Division, National Technical University of Athens, Greece*

**ABSTRACT:** The seismic response of shallow foundations on liquefiable sand is studied herein through fully coupled effective stress analyses. The numerical methodology that is used, is based on a bounding surface model for non-cohesive soils implemented into the Finite Difference code FLAC2D. Model constants are calibrated against element laboratory tests on Nevada sand, while the simulation of centrifuge model tests of the VELACS project validates the User-Defined Model's performance on boundary value problems. Using this well established methodology, parametric analyses are performed, for the common case of a thin clay cap overlying a liquefiable sand layer, in order to provide insight to the mode of failure and the mechanism of settlement accumulation. It is shown that groundwater flow during and immediately after shaking affects the response, while there is a "critical thickness" of the clay cap beyond which sand liquefaction does not lead to bearing capacity degradation is also evaluated.

## 1 INTRODUCTION

Estimation of the seismic response of shallow foundations during a strong earthquake has been proven a difficult task throughout the years. The main cause of this difficulty arises from the fact that soil behaves in a highly non-linear manner when subjected to large cyclic strains. It can deform substantially and, when saturated, can develop high pore pressures and finally liquefy. Liquefaction consequently leads to severe loss of bearing capacity, which damages seriously the superstructure. Extensive damage to shallow foundations due to liquefaction has been reported in numerous cases in the past, from Niigata (1964) earthquake to the more recent 1999 M 7.4 Kocaeli earthquake.

Despite the severity of damages, relatively little has been achieved towards the development of a consistent methodology for the design of foundations systems under these circumstances. Usually, the presence of superstructure is neglected and calculations are performed for free-field conditions. The onset of liquefaction is evaluated and empirical correlations for settlements, developed for free-field conditions, are used. However, the presence of superstructure differentiates significantly the response from that under free-field conditions, so that such methods prove too approximate.

The complicated response of soil-structure system is studied herein through a fully coupled effective stress analysis. Using a recently developed numeri-

cal methodology, the common case of a non-liquefiable clay cap overlying a liquefiable sand layer is investigated through parametric analysis.

The research focuses upon three crucial questions for the development of a design methodology:

- The shape of the failure surface, when the sand layer liquefies
- The critical thickness of the clay cap beyond which sand liquefaction does not affect foundation system
- The role of sand permeability and groundwater flow

Findings of this research are compared with those of an analytical methodology, originally proposed by Cascone & Bouckovalas (1998) and extended by Bouckovalas et al. (2005), for the pseudo-static evaluation of seismic bearing capacity of footings on liquefiable soil.

## 2 NUMERICAL METHODOLOGY

The cornerstone of the numerical methodology used herein is a recently developed bounding surface model for non-cohesive soils which is implemented to FLAC (Itasca, 2005) using its UDM (User-Defined Model) capability (Andrianopoulos et al., 2006). This new UDM is a bounding surface model with a vanished elastic region that incorporates Critical State Theory.

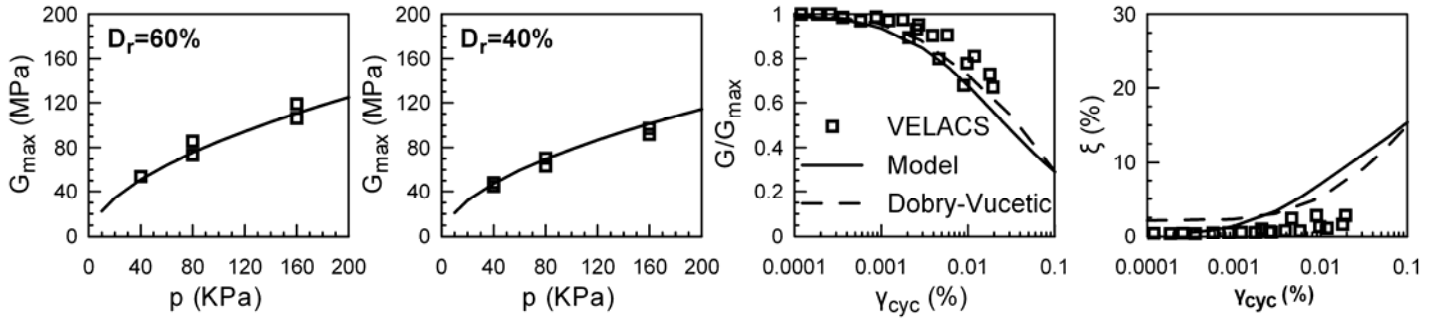


Figure 1. Summary comparisons of simulations versus laboratory data for cyclic shearing in terms of  $G_{max}$ ,  $G/G_{max}-\gamma_{cyc}$  and  $\xi-\gamma_{cyc}$ .

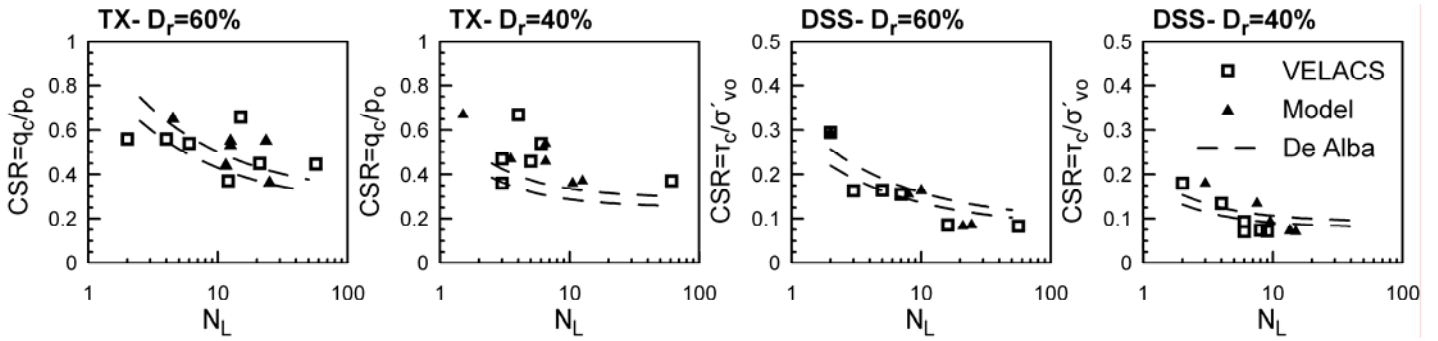


Figure 2. Summary comparisons of laboratory data versus simulations for cyclic shearing in terms of the number of cycles  $N_L$  to initiate liquefaction.

It is based on a recently proposed model (Papadimitriou et al. 2001, Papadimitriou & Bouckovalas 2002), and has been developed with the ambition to simulate the cyclic behavior of non-cohesive soils under various (small – medium- large) cyclic strain amplitudes, initial stress and density conditions, using a single set of parameters.

In its current form, the model incorporates three open cone-type surfaces with apex at the origin of stress space: (i) the critical surface, (ii) the bounding surface and (iii) the dilatancy surface. Its basic feature is the direct association of shear behavior to the state parameter  $\psi$  (Been and Jefferies, 1985), which is defined with respect to a unique critical state line (CSL) or steady state line. The non-linear soil response under small to medium cyclic strain amplitudes is simulated mainly by introducing a Ramberg-Osgood type hysteretic formulation.

The aforementioned constitutive model was incorporated to the commercial code FLAC, using the UDM option. To ensure numerical stability, the substepping technique with automatic error control (Sloan et al. 2001) was adopted, which belongs to the family of effective explicit algorithms.

The model was calibrated against data from element laboratory tests performed on fine Nevada sand at relative densities of  $D_r = 40\%$  and  $60\%$  and initial effective stresses between 40 and 160 kPa (Arulmoli et al. 1992). In particular, the data originate from resonant column tests as well as undrained cyclic direct simple shear and triaxial tests. Thus, they offer a quantitative description of various aspects of non-cohesive soil response under cyclic loading, such as

shear-modulus degradation and damping increase with cyclic shear strain, liquefaction resistance and cyclic mobility. Results from this calibration are presented in Figures 1 - 2.

The numerical methodology has been consequently validated against results from the well known VELACS experimental project (Arulmoli et al. 1992). In that effect, results from centrifuge tests No. 1 and No. 2 were originally used, simulating the one-dimensional (1-D) response of a liquefiable soil under level and mildly sloping sites respectively.

Furthermore, centrifuge test No. 12 was used, which simulates the more complex response of shallow foundations on liquefiable sand layer, underlain a non-liquefiable crust. The results from the latter validation are presented in Figures 3 and 4. The comparisons are made in terms of excess pore pressures, accelerations and displacement time histories, at the vicinity of the structure as well as at the free-field. Further details from this comparison can be found at Andrianopoulos et al. (2006). As it is observed, the numerical methodology predicts reasonably well the measured response.

### 3 PARAMETRIC ANALYSES

#### 3.1 Problem description

The common case of a strip foundation resting on a non-liquefiable clay crust, overlaying a liquefiable sand layer, is examined parametrically. The clay cap corresponds to an overconsolidated clay with undrained shear strength  $c_u = 40kPa$ ,

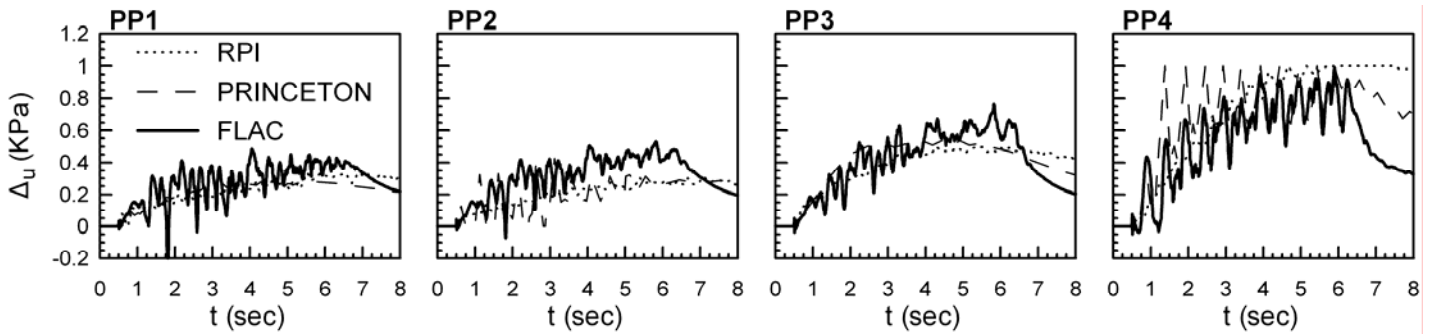


Figure 3. Excess pore pressure ratio time histories.

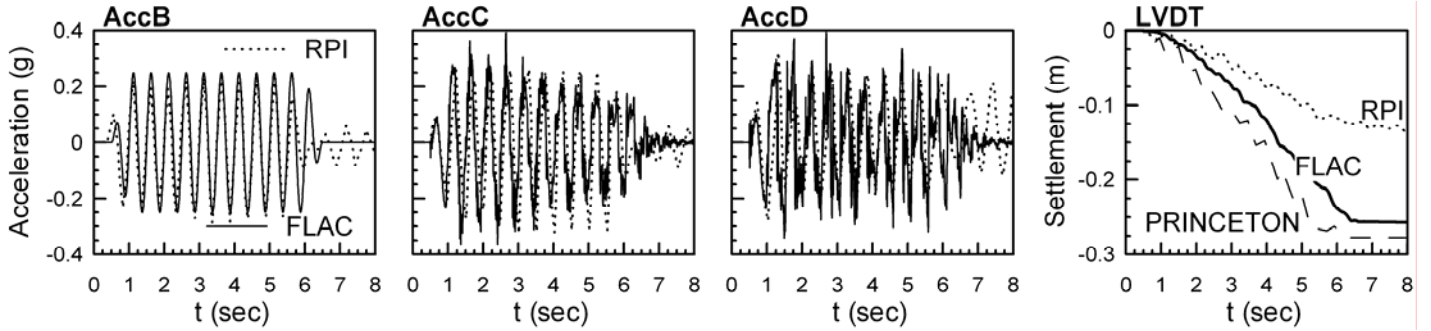


Figure 4. Acceleration and settlement time histories

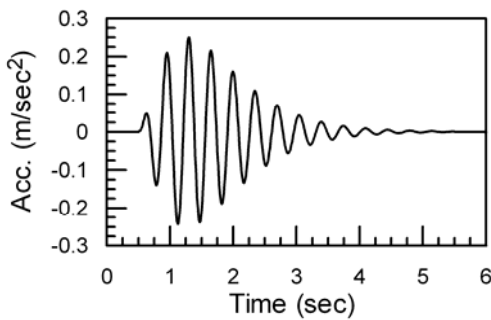


Figure 5. Input motion.

while the sand layer refers to a liquefiable fine-grained sand of relative density  $D_r = 50\%$ . The permeability of the sand layer is assumed equal to  $2.1 \times 10^{-3}$  cm/sec, while the clay cap is assumed practically impermeable, i.e. with permeability equal to  $1 \times 10^{-7}$  cm/sec

The width of the foundation is taken as  $B=4m$ , while the thickness of the clay cap  $H$  is variable. The foundation system corresponds to a rigid foundation. Inertia effects are neglected. Furthermore, the model is subjected to a dynamic excitation, applied on the base of the sand layer. The input motion consists of a Chang's signal with peak acceleration equal to  $0.25g$ , and shaking time approximately 3 sec (Figure 5).

The numerical results presented herein, are commented in connection with a simple pseudo-static approach presented earlier by Cascone and Bouckovalas (1998) and refined by Bouckovalas et al. (2005), for the design of shallow foundations at liquefiable regimes. Based on analytical solutions for shallow footings on a two layered soil, proposed by Meyerhof and Hanna (1978), this methodology com-

putes the post-seismic static bearing capacity, taking into account the average excess pore pressure ratio that is expected to develop under the footing at the end of shaking. The correction coefficients are computed as a function of initial soil properties, geometry of the footing and soil profile. Also, the minimum required thickness of the clay cap is estimated, so that liquefaction does not affect the bearing capacity.

### 3.2 Simulation details

The width of the mesh used for the analyses, was  $60\text{ m} (=15B)$ , while the total simulated depth equals  $20\text{ m}$ . The elements used varied from (width x thickness)  $1\text{ m} \times 1\text{ m}$  under the footing to  $2\text{ m} \times 1\text{ m}$  at the free field.

The bottom nodes were fixed in both horizontal and vertical direction. 'Tied-node' boundary conditions were considered for the lateral boundaries, by restraining the horizontal displacements of the corresponding nodes on the left and right boundary to have the same value. All boundaries were considered impermeable, apart from the top boundary where inflow and outflow were allowed.

The sand layer was modeled using the previously described UDM, while the inbuilt Mohr-Coulomb model ( $c_u=40\text{ KPa}$ ,  $\phi=0$ ) was used for the non-liquefiable clay crust. Three different clay cap thicknesses were examined, namely  $H=B$ ,  $2B$  and  $3B$  (i.e.  $4\text{ m}$ ,  $8\text{ m}$  and  $12\text{ m}$ , respectively). In all cases, water level was assumed to be located  $1\text{ m}$  above the soil surface, in order to ensure saturated conditions.

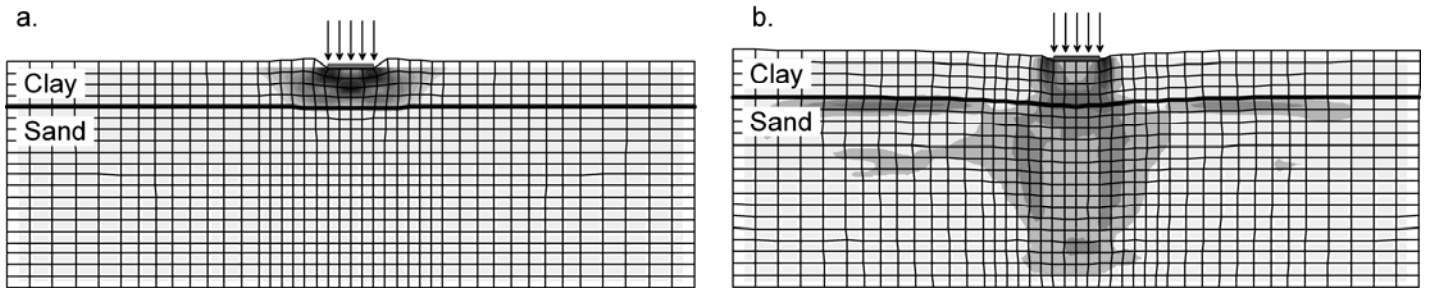


Figure 6. Deformed mesh, shear strain increment contours and displacement vectors indicating the mode of (a) static and (b) dynamic failure.

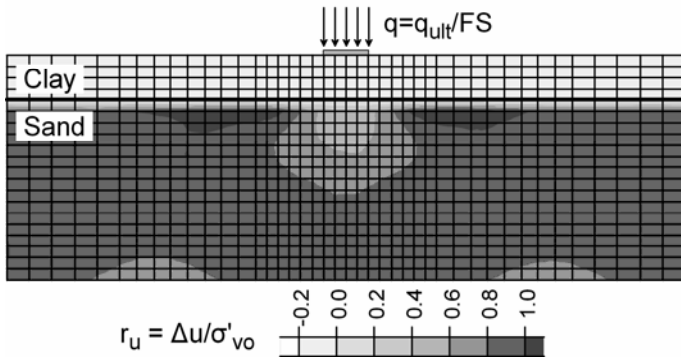


Figure 7. Excess pore pressure ratio contours at  $t=5.0\text{sec}$ .

The foundation was considered rigid and totally bonded to the soil. The analyses were performed in two (2) stages.

- The foundation was first loaded statically, with a uniform surcharge load (130KPa). This value corresponds to a static factor of safety equals to 2, for the case of clay cap thickness  $H=B$  ( $q_{ult,cs}^{H=B} = 260 \text{ kPa}$ )
- Then, the model was subjected to dynamic excitation. During the dynamic analyses, groundwater flow was coupled to mechanical behavior.

### 3.3 Mode of failure

Figure 6 compares the deformed mesh and the contours of shear strain increments for two different modes of failure, namely failure for static loading equal to the ultimate bearing capacity and failure at the end of shaking, considering an initial static safety factor of 2.

Focusing in Figure 6a, failure due to static loading is shown to occur inside the clay cap. On the other hand, Figure 6b shows that the mechanism of failure after liquefaction of subsoil, is quite different. A punch-through type of failure is observed within the clay cap and the underlying sand, where the shear strain rate contours indicate the formation of an orthogonal prism underneath. Liquefaction of the surrounding soil seems to reduce this block's lateral support and result in the accumulation of large vertical strains. In fact, for the case of  $H=B=4\text{m}$ , liquefaction of the sand layer resulted in the development of settlements equal to 15.6cm.

The above failure mechanism due to liquefaction, resembles the one assumed by the analytical method of Bouckovalas et al. (2005), where the bearing capacity of the sand layer degrades gradually as a function of pore pressures development. Furthermore, this type of failure has been observed in numerous earthquakes, and is typical of relatively low height over width ratio buildings, which settle almost vertically with little deviation from verticality.

Proceeding further to the investigation of the failure mechanism, Figure 7 provides insight to the evolution of excess pore pressures during shaking. Namely, contours of excess pressure ratio  $r_u = \Delta u / \sigma'_{vo}$  are presented at the end of shaking ( $t=5\text{sec}$ ). Note that excess pore pressure ratio  $r_u$  is an index of proximity to liquefaction, normalizing excess pore pressures  $\Delta u$  developed during shaking to the initial effective vertical stress  $\sigma'_{vo}$ . Values of  $r_u$  close to 1 indicate liquefaction of the subsoil.

It is clearly shown that the presence of the foundation, and the resulting increase of soil stresses underneath it, significantly differentiates the response from the free-field conditions.

Developed excess pore pressures inside the sand layer, immediately below the foundation, are not able to reduce the effective stresses to zero, and hence no liquefaction is observed. Also, at the perimeter of the superstructure, the increase of initial shear stresses, without an equivalent increase of the mean effective stresses, brings the subsoil closer to failure, and hence closer to liquefaction. This observation, accompanied with migration of water from the axis of foundation to free-field, potentially explains the presence of liquefied soil at the perimeter of foundations, that has been observed in numerous earthquakes. These effects of the superstructure are usually neglected in current practise.

Figure 8 compares the excess pore pressure ratio time histories developing at several depths underneath the footing and at the free field, as well as the recorded settlements. Even though the values of  $r_u$  remain close to 1 at the free field, at the axis of foundation and 1.5m below the clay cap (5.5m below the soil surface) the excess pore pressure ratio remains lower than 0.6 during shaking. Moving to larger depths, normal and shear stresses applied from the footing are reduced, and excess pore pressure ratios

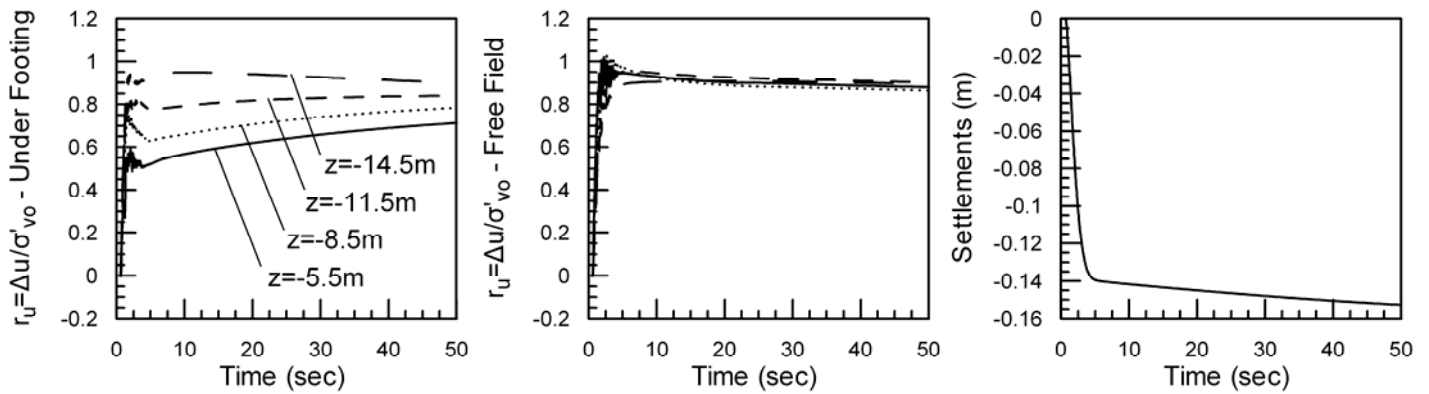


Figure 8. Long-term evolution of excess pore water pressures (at various depths underneath the footing and in the free field) and foundation settlements.

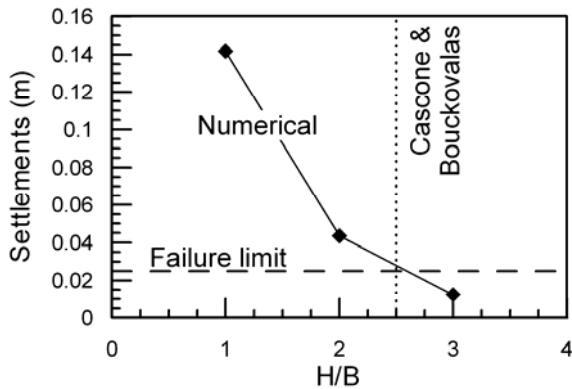


Figure 9. Comparison of the evolution of dynamic settlements for different clay cap thicknesses and variation of the final settlements with  $H/B$ .

tend to become equal to the ones developing in the free field.

This variation of pore pressures with depth initiates vertical upward flow, resulting to a long term increase of the excess pore pressure ratio under the footing, as clearly shown in Figure 8. On the other hand, excess pore pressures in the free field remain high, because of the existence of the relatively impermeable clay cap. It is noticed, though, that footing settlements continue to increase at a slow rate during the consolidation process. This is attributed to the redistribution of excess pore water pressures underneath the foundation. However, the long term settlements (1.6cm) are generally smaller compared to the ones developing during shaking (14cm).

### 3.4 Evaluation of 'critical depth'

From a practical point of view, a crucial question to answer is whether a critical thickness of non-liquefiable layer exists, beyond which liquefaction of the underlying layer does not affect the superstructure. On that purpose, two more analyses were performed, considering different clay cap thicknesses, i.e.  $H = 8$  &  $12$ m. Results from these analyses are presented at Figure 9, where the estimated foundation settlement is correlated with the ratio of cap thickness to the width of foundation  $H/B$ . Settlements due to excess pore pressure buildup are

greatly reduced, with the increasing cap thickness. This finding is in agreement with the "critical depth", obtained by the pseudo-static approach of Cascone & Bouckovalas (1998) and Bouckovalas et al. (2005). Note that the analytical solution predicts  $(H/B)_{cr} = 2.00 \div 2.50$  when mean  $r_u$  ranges from 0.7 to 1.0, as in the case of Figure 7.

### 3.5 Effect of groundwater flow and permeability

Figure 10 presents results for two different values of sand permeability, i.e.  $2.1 \times 10^{-4}$  m/sec and  $2.1 \times 10^{-5}$  m/sec (basic run). Both analyses predict similar response during shaking, indicating that, for these permeability values, flow is not significant during shaking and does not affect practically the results.

However, immediately after shaking, water flow from deeper to shallower layers affects greatly the computed response. Namely, an increase of excess pore pressure ratios is observed that leads to a further increase of foundation settlements. This is most prominent for the case of  $k = 2.1 \times 10^{-4}$  m/sec, where flow occurs at faster rate. In the case of a less permeable sand layer (i.e.  $k = 2.1 \times 10^{-5}$  m/sec), the change of pore pressures and settlements due to water flow, takes place at a slower rate.

Note also that, although the total value of displacement remains practically the same for both cases (15.6cm at  $t=50$ sec), post-shaking settlements become greater part of the total displacements as soil permeability decreases, i.e. 10% for  $k=2.1 \times 10^{-5}$  m/sec compared to 6% for  $k=2.1 \times 10^{-4}$  m/sec. This phenomenon has also been observed in centrifuge studies (Liu and Dobry, 1997) and explains partly the delayed failure of foundation systems, observed in earthquakes where fine-grained soils have been liquefied (e.g. Adapazari, 1999).

## 4 CONCLUDING REMARKS

The seismic response of shallow foundations on liquefiable sand is studied herein through fully coupled effective stress analysis. The common case of a



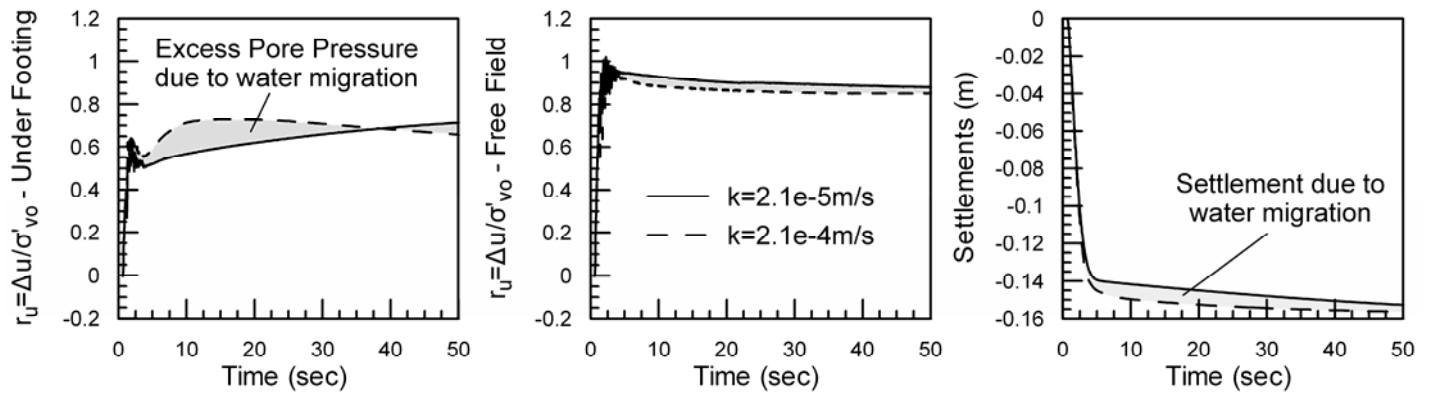


Figure 10. Comparison of dynamic analysis with different permeabilities, in terms of excess pore pressure ratio under the footing and in the free field and foundation settlements.

non-liquefiable clay cap overlying a liquefiable sand layer is explored. On that purpose, a recently developed numerical methodology is used, that consists of a bounding surface model for non-cohesive soils, implemented in FLAC. The findings of this research are compared with those of a pseudo-static approach for the design of foundations where liquefaction occurs. As concluded from the parametric runs presented:

- Effective stress analysis can be used to analyze and explore significant aspects of dynamic soil-structure interaction and liquefaction phenomena
- The presence of superstructure affects greatly the response of the subsoil, differentiating it from the free-field response
- A “critical depth” of clay cap exists, beyond which, liquefaction of the subsoil does not damage the foundation
- Groundwater flow, immediately after the end of shaking, redistributes pore pressures, leading to a delayed increase of foundation settlements.
- For commonly used static factors of safety (e.g. 2), foundation settlements due to liquefaction can be excessive.

## 5 ACKNOWLEDGMENTS

The work presented herein has been financially supported by the General Secretariat for Research and Technology (Γ.Γ.Ε.Τ.) of Greece, through research project EIIAN – ΔΠ23 (“X-SOILS”). This contribution is gratefully acknowledged.

## REFERENCES

- Andrianopoulos K. I., Papadimitriou A. G., Bouckovalas G.D. (2006), “Implementation of bounding surface model for seismic response of sands”, 4<sup>th</sup> International FLAC Symposium, Proceedings (to appear)
- Arulmoli K., Muraleetharan K. K., Hossain M. M., Fruth L. S. (1992), “VELACS: verification of liquefaction analyses by centrifuge studies; Laboratory Testing Program – Soil Data

- Report”, Research Report, The Earth. Technology Corporation
- Been K. & Jefferies M.G. (1985), “A state parameter for sands”, *Geotechnique*, 35 (2), pp. 99-112
- Bouckovalas G.D, Valsamis A. I., Andrianopoulos K. I. (2005), “Pseudo static vs performance based seismic bearing capacity of footings on liquefiable soil”, Proceedings of the TC4 Satellite Confer., 16<sup>th</sup> ICSMGE, Osaka, pp. 22-29
- Cascone E. & Bouckovalas G. (1998), “Seismic bearing capacity of soils”, Proceedings 11<sup>th</sup> European Conference in Earthquake Engineering, Paris, September
- Liu L. & Dobry R. (1997), “Seismic response of shallow foundation on liquefiable sand”, *Journal of Geotech. & Geoenviron. Engrg.*, ASCE, Vol. 123 (6), pp. 557 -567
- Papadimitriou A. G., Bouckovalas G. D., Dafalias Y. F. (2001), “Plasticity model for sand under small and large cyclic strains”, *J. Geotech. Geoenviron. Engrg.*, ASCE, Vol. 127 (11), pp. 973-983
- Papadimitriou A. G., Bouckovalas G. D. (2002), “Plasticity model for sand under small and large cyclic strains: a multi-axial formulation”, *Soil Dynamics and Earthquake Engineering*, Vol. 22, pp. 191-204
- Sloan S. W., Abbo A. J., Sheng D. (2001), “Refined explicit integration of elastoplastic models with automatic error control”, *Engineering Computations*, Vol. 18(1/2), pp. 121-154
- Itasca (2005), “Fast Lagrangian Analysis of Continua”, Version 5
- Meyerhoff G.G. & Hanna A.M. (1978), “Ultimate bearing capacity of foundations on layered soils under inclined load”, *Canadian Geotechnical Journal*, Vol. 15 (4), pp. 565-572